

De Sitter Special Relativity as a Possible Reason for Conformal Symmetry and Confinement in QCD

M. Kirchbach¹, C. B. Compean²

¹ Instituto de Física, UASLP, Av. Manuel Nava 6, Zona Universitaria,
San Luis Potosí, S.L.P. 78290, México

² Instituto Tecnológico de San Luis Potosí,
Av. Tecnológico S/N col. UPA,

Soledad de Graciano Sánchez near San Luis Potosí, S.L.P. 78437, México

Abstract

Conformal symmetry and color confinement in the infrared (near rest-frame) regime of QCD are attributed to the global properties of a four-dimensional (4D) space-time of a deSitter dS_4 geometry which, according to the principle of deSitter special relativity, is viable outside the causal Minkowski light cone, where it reigns over the interactions involving the virtual gluon- and quark degrees of freedom of hadrons. Within this scenario, the conformal symmetry of QCD is a direct consequence of the conformal symmetry of the dS_4 space-time, while the color confinement appears as a consequence of the innate charge neutrality of the unique closed space-like geodesic on this space, the three dimensional hypersphere S^3 , also being the unique dS_4 sub-manifold suited as a stage for near rest-frame physics. In further making use of the principles of the mathematical discipline of potential theory, and postulating that fundamental interactions are defined by Green functions of Laplace operators on manifolds, taken here as the dS_4 geodesics, a color-dipole potential has been derived on S^3 whose magnitude, $N_c \alpha_s$, is the product of the number of colors, N_c , and the strong coupling constant α_s in QCD, and pretty much as the amplitude, $Z\alpha$ of the Coulomb interaction following from QED. Hadrons now present themselves as light quarkish color-anticolor “dumbbells” in free 4D rotations around their mass centers, equivalent to inertial quantum motions along S^3 , possibly slightly perturbed by the color-dipole potential from above, attributed to a 4D gluon-anti-gluon “dumbbell”, sufficiently heavy to remain static to a good approximation. A description of the spectra of the unflavored mesons within the above scenario allows to extract the α_s/π value, which we obtain to vary between 0.58 and 0.8, and in accord with data extracted from the spin structure function.

PACS: 03.30.+p (Special relativity), 11.30.-j (Symmetry in theory of fields and particles), 12.38.Aw (Quark confinement)

Key words: deSitter special relativity, conformal symmetry, color confinement, unflavored mesons, strong coupling constant value

“Think geometrically, prove algebraically”,
John Torrence Tate Jr.
“...verify experimentally!”
Galileo

1 Introduction

Theoretical models in physics are frequently developed with the aim to explain particular observational data. Such an approach, termed to as “bottom-up”, obviously depends on the choice of the data set. It can happen that at different energy scales, different models can be adequate. For example, at low-, up to pretty high energies, the electron charge in the Quantum Electrodynamics (QED) can be considered as a constant, but in very strong electromagnetic fields, as generated in the interiors of stars, it can become dependent on the momentum transferred in collisions. Particles interacting via the so called “strong” interactions, the hadrons, are described in analogy to QED by a properly designed fundamental (gauge) theory, the Quantum Chromodynamics (QCD), named in this way in reference to the hypothesis that the hadron constituents, the quarks, are endowed with three different “charges”, conditionally termed to by color names as “red”, “blue”, and “green”. All strong interacting systems observed so far have been found to be color-neutral, a phenomenon known as color-non-observability, or, color confinement. The phenomenon has been built into the fundamental (gauge) theory of strong interactions

through a special choice of the so called gauge group, denoted by $SU(3)_c/Z_3$, which first prescribes the number of “colored” photons, the gluons, to be eight, and then “locks” the color degrees of freedom. The space-time wave equations following from QCD are differential equations of high order and difficult to tackle. For the immediate analyzes of the rapidly accumulating data on hadrons referring to their masses, decay modes, collision probabilities (scattering cross sections), compiled in [1], a model has been developed, the so called “constituent” quark model which is based on second order differential equations of the Sturm-Liouville type, equivalent to quantum mechanical wave equations of the Schrödinger-, Klein-Gordon-, or Dirac kind with potentials. The point of departure for the traditional quark model [2] have been the particles of the lowest masses, the so called pseudo-scalar mesons, the pions (π), kaons (K), and the η , on the one side, and the spin-1/2 baryons, the nucleon (N), the Σ and Ξ hyperons, as well as their spin-3/2 excitations Δ , Σ^* , and Ξ^* , supplemented by a new particle, the so called Ω hyperon. The potentials of conventional use employed so far within this framework have been predominantly power potentials. As a rule, the quark models can not be directly linked to the gauge theory of strong interactions, possibly with the exception of the MIT bag model [3], and versions of it [4]. To the best of our knowledge, none of the conventional constituent quark models has provided hints on possible reasons behind the confinement, nor a prediction on the value of the fundamental color charge in the QCD. In a recent work, the choice of the data set to be explained by a “bottom-up” quark model has been shifted from the lowest to the highest masses of the unflavored mesons which are of the order of 2300 MeV. The phenomenon to be explained there refers to striking degeneracies between states distinct through their spins but of same isospin (number of states with different electric charges), and same CP quantum numbers (the product of spatial (P), and charge conjugation (C) parities). A possible explanation has been suggested in [5] on the basis of two principles. We assumed validity of the

- principle of deSitter special relativity [6] outside of the causal light cone in the traditional Einsteinian special relativity,
- principle of the mathematical discipline of potential theory, according to which instantaneous fundamental interactions are defined by Green functions of Laplace operators on manifolds [7], taken as the dS_4 geodesics, in our case.

Within such a scenario it becomes possible to derive from first principles a strong potential whose magnitude, $N_c\alpha_s$, is given by the product of the number of colors, N_c , with the fundamental strong coupling constant, α_s , in OCD, pretty much as the magnitude, $Z\alpha$, of the Coulomb potential perceived by an electron is given by the product of the number of electric charges, Z , of the source, with the fundamental constant α of QED. The strong potential derived in this way allows to put the description of mesons, the simplest composite (two-body) system in QCD, at comparable footing with that of the H Atom, the simplest composite (two-body) system in QED. In fitting data on the observed degeneracy patterns of the unflavored meson spectra by the above potential, a prediction for α_s can be obtained, a point that remained unaddressed in [5] and will be attended in the following.

In the present study we first highlight the proposal of [5] and then put it at work with the aim to extract here for the first time the α_s value from data on meson spectra. The article is structured as follows. In the next section we present the idea of [6] on the extension of the Einsteinian special relativity toward deSitter relativity outside the causal light cone. In section 3 we build up the algebraic description of the deSitter geometry, which allows us to consider there free quantum motions on the respective unique closed hyper-spherical space-like geodesic, and the open hyperbolic time-like geodesics. In section 4 we transform these two free motions on the deSitter space-time into quantum mechanical wave equations with centrifugal potentials taking the shape of the trigonometric Scarf well-, and the hyperbolic Pöschl -Teller potentials, respectively, and present a scenario for a duality between the low-energy(infrared) and the ultra-high energy (ultraviolet) regimes of QCD. In section 5 we explore consequences of the innate charge neutrality of the hypersphere on the structure of systems living on this space and derive on the basis of potential theory a picture of confinement and the internal structure of the mesons that is testable through data. In section 6 we analyze data on the f_1 and a_1 meson masses and combine them with the corresponding data on the π , a_0 , η , and f_0 mesons, earlier classified in [5]. Finally, in section 7 we extract the α_s value from studying a total of 89 meson masses, before closing with a short Summary and Outlook section.

2 The Geometric Ansatz. Immersing Minkowski- into deSitter space-time

All theoretical descriptions of processes in the micro-world have to obey the theory of Special Relativity which requires the values of the physical observables to be same in all coordinate frames related to each other by the Lorentz transformations which, besides translations, conserve the “intervals”, s^2 , in a Minkowskian space-time of one time-like (ct) and three space-like (\mathbf{r}) dimensions according to,

$$(ct)^2 - \mathbf{r}^2 = c^2(t_1 - t_2)^2 - (x_1 - x_2)^2 - (y_1 - y_2)^2 - (z_1 - z_2)^2 = s^2, \quad s^2 \geq 0, \quad \text{or} \quad s^2 \leq 0. \quad (1)$$

Here, x_i , y_i , and z_i (with $i = 1, 2$) are the Cartesian position coordinates of two points in ordinary three dimensional Euclidean space, t_1 and t_2 are in their turn the time coordinates, and c is the speed of light. The very first fundamental theory known to remain invariant under Lorentz transformations is Maxwell’s electrodynamics. For a comparatively long period this fact has been considered as some peculiarity of the electric and magnetic interactions between moved bodies. This changed with Einstein’s seminal work [9] in which the speed of light has been postulated to remain same in all reference frames moving uniformly on parallel straight lines relative to each other. This scenario rules out the Euclidean space time inherent to the classical low-velocity mechanics, and replaces it by the Minkowskian space time that defines a new mechanics at high velocities, the relativistic mechanics. In this way, the importance of Lorentz invariance was shifted from the particular case of electrodynamics to the principle properties of space-time and made mandatory for all theories formulated there. From this moment on, the structure of space-time acquired fundamental importance in physics. The intervals in (1) can be viewed as genus-es of points lying on three dimensional two-sheeted hyperboloids, denoted by \mathbf{H}_\pm^3 , encapsulated inside the “null hyperboloid”, $c^2t^2 - \mathbf{r}^2 = 0$, a cone also termed to as the “Light Cone”, as schematically illustrated in Fig. 1. The null-intervals remain invariant under five more transformations termed to as “conformal”, the resulting symmetry being the “conformal symmetry” [10]. The conformal symmetry is associated with all the transformations which leave the interval, $ds^2 = g_{\mu\nu}(x)dx^\mu dx^\nu$, invariant, modulo a multiplicative “conformal factor” of $e^{\omega(x)}$. Such transformations are angle- but not distance preserving.

In thinking geometrically, one can ask the question, posed in [6], on the type of physics one could encounter by imagining the light cone and the enclosed \mathbf{H}_\pm^3 hyperboloids immersed into a four-dimensional hyperboloid of one sheet as schematically represented in Fig. 2 on the left. Stated differently, one could entertain the idea of extending the inaccessible to direct measurements space-like region by one more space-like dimension, x_4 , and requiring outside the causal region invariance of intervals in the larger five-dimensional space-time,

$$c^2t^2 - \mathbf{r}^2 - x_4^2 = s^2, \quad s^2 = -R^2 < 0, \quad (2)$$

with the choice of $ct_2 = x_2 = y_2 = z_2 = 0$, $ct_1 = ct$, $x_1 = x$, $y_1 = y$, $z_1 = 1$, and R being a real length parameter. A space-time defined in this way is known under the name of “four-dimensional deSitter space-time”, abbreviated, dS_4 . It represents a four dimensional hyperboloid of one sheet, denoted by \mathbf{H}_1^4 , with a time-like symmetry axis. Within this set up, causal hyperboloids in Einstein’s special relativity correspond to so called causal patches on dS_4 obtained through intersections of this space-time by four-dimensional planes parallel to the symmetry axes, so called slicing, as shown in Figure 2 on the right. The interval in (2) is conserved besides under Lorentz transformations also under transformations which ensure the transitivity of the dS_4 space-time and combine in a particular way translations with four of the five conformal transformations, the so called proper conformal transformations, a reason for which dS_4 features conformal symmetry [6].

3 Building up the algebraic description of the dS_4 geometry

In this section, which partially follows our previous work [5], we aim to motivate usefulness of the dS_4 geometry for quantum physics. For this purpose we start building up the algebraic description of quantum motions there, beginning with free motions. Free quantum motions on any space-time are described by the eigenmodes of the kinetic energy operator there, given by the respective Laplacian. On dS_4 , parametrized in global coordinates as

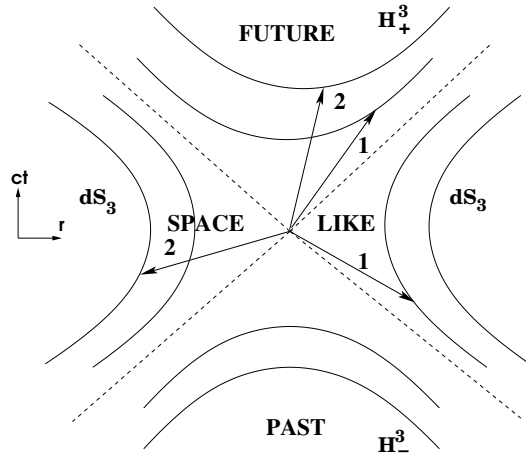


Figure 1: Schematic presentation of the Minkowskian space time on the plane. Two examples of moved reference frames are given, their axes being labeled by “1”, and “2”. The axes of a frame in motion do not remain mutually orthogonal, the angle between them being dependent on the velocity. Intervals with $s^2 > 0$ define the foliation of the Minkowski space-time with three-dimensional hyperboloids of two sheets (marked by H_{\pm}^3), all symmetric with respect to the vertical time axis. For $s^2 < 0$ the foliation requires three-dimensional hyperboloids of one sheet, so called deSitter dS_3 space-times. The dashed lines mark the light cone. In Special Relativity it is shown that the hyperboloids of two sheets are causal meaning that the time-ordering (“before-after”) is preserved by all Lorentz transformations, while the surrounding hyperboloid of one sheet represents the acausal region, where Lorentz transformation can change the time-orderings but conserve the space-orderings (“near-far”). Measurements in physics are possible only in the causal region, and the processes are termed to as “real”, or “on-shell”, in reference to the definition of the invariant mass, M , by means of the so called “mass-shell” relation, $E^2 - \mathbf{p}^2 = M^2$, between its energy, E , and linear momentum, \mathbf{p} . The hyperboloids inside the upper part of the cone describe the causal “Future” while those of the down part describe the causal “Past”. The “space-like” region outside the light cone describes interactions by means of instantaneous potentials, in reference to the fact that instantaneity, in not allowing for time-ordering, violates causality. Processes here are termed to as “virtual”, or “off-shell”.

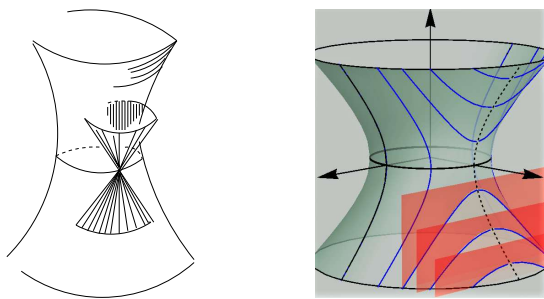


Figure 2: The causal Minkowski light cone relevant to a local observer on dS_4 (left) as a causal patch obtained through dS_4 intersection by a four-plane parallel to the time-axis (right). On the left figure the hyperboloid of one sheet has to be thought of as having one space-like dimension more than the light cone.

[11],

$$\begin{aligned}
x^0 &= R \sinh \rho, \quad \rho \in (-\infty, +\infty), \\
x^4 &= R \cosh \rho \sin \chi, \quad \chi \in \left[-\frac{\pi}{2}, +\frac{\pi}{2}\right], \\
x^1 &= R \cosh \rho \cos \chi \sin \theta, \quad \theta \in \left[-\frac{\pi}{2}, +\frac{\pi}{2}\right], \\
x^2 &= R \cosh \rho \cos \chi \cos \theta \sin \varphi, \quad \varphi \in [0, 2\pi], \\
x^3 &= R \cosh \rho \cos \chi \cos \theta \cos \varphi,
\end{aligned} \tag{3}$$

one encounters the Laplacian, denoted by $\Delta_{dS_4}(\rho, \chi, \theta, \varphi)$ as,

$$\Delta_{dS_4}(\rho, \chi, \theta, \varphi) = \frac{1}{R^2 \cosh^3 \rho} \frac{\partial}{\partial \rho} \cosh^3 \rho \frac{\partial}{\partial \rho} + \frac{\mathcal{K}^2(\chi, \theta, \varphi)}{R^2 \cosh^2 \rho}. \tag{4}$$

Here, $\mathcal{K}^2(\chi, \theta, \varphi)$ stands for the squared four dimensional angular momentum operator, given by

$$\mathcal{K}^2(\chi, \theta, \varphi) = -R^2 \Delta_{S^3}(\chi, \theta, \varphi) = -\frac{1}{\cos^2 \chi} \frac{\partial}{\partial \chi} \cos^2 \chi \frac{\partial}{\partial \chi} + \frac{\mathbf{L}^2(\theta, \varphi)}{\cos^2 \chi}, \tag{5}$$

where $\Delta_{S^3}(\chi, \theta, \varphi)$ is now the Laplace operator on the unique closed space-like geodesic [12] on dS_4 which is a three dimensional hyper-sphere, S^3 , of (hyper)radius R . The $\Delta_{dS_4}(\rho, \chi, \theta, \varphi)$ free waves are then described in terms of five-dimensional pseudo-spherical harmonics, denoted by $Y_{\bar{K}K\ell m}(\rho, \chi, \theta, \varphi)$, the solutions to

$$-\hbar^2 c^2 \Delta_{dS_4}(\rho, \chi, \theta, \varphi) Y_{\bar{K}K\ell m}(\rho, \chi, \theta, \varphi) = -\frac{\hbar^2 c^2}{R^2} \bar{K}(\bar{K} + 3) Y_{\bar{K}K\ell m}(\rho, \chi, \theta, \varphi). \tag{6}$$

Here, \bar{K} can take all non-negative integer values, while K, ℓ and m , obey the branching rules, $K = \bar{K} + n_r = 0, 1, 2, \dots, \infty$, $\ell \in [0, K]$, $|m| \in [0, \ell]$. They stand in turn for the four-, three-, and two-dimensional angular momentum values labeling the eigenmodes of the squared angular momentum operators in four-, three, and two Euclidean dimensions, respectively. Furthermore, the five dimensional pseudo-spherical harmonics, $Y_{\bar{K}K\ell m}(\rho, \chi, \theta, \varphi)$, express as,

$$Y_{\bar{K}K\ell m}(\rho, \chi, \theta, \varphi) = \phi_{\bar{K}}(\rho) Y_{K\ell m}(\chi, \theta, \varphi), \tag{7}$$

$$Y_{K\ell m}(\chi, \theta, \varphi) = S_{n\ell}(\chi) Y_{\ell}^m(\theta, \varphi), \tag{8}$$

$$S_{n\ell}(\chi) = \cos^{\ell} \chi \mathcal{G}_n^{\ell+1}(\sin \chi), \quad n = K - \ell, \tag{9}$$

with $Y_{K\ell m}(\chi, \theta, \varphi)$, $\mathcal{G}_n^{\ell+1}(\sin \chi)$, and $Y_{\ell}^m(\theta, \varphi)$ in turn denoting the four-dimensional (hyper)spherical harmonics, the Gegenbauer polynomials, and the ordinary spherical harmonics.

On their side, the $\phi_{\bar{K}}(\rho)$ functions in (7) express in terms of Jacobi polynomials, $P_{n_r}^{ab}(x)$, of equal real parameters, and a pure imaginary argument according to,

$$\phi_{\bar{K}}(\rho) = \cosh^{-\frac{a}{2} - \frac{3}{2}} \rho P_{n_r}^{-a - \frac{1}{2}, -a - \frac{1}{2}}(i \sinh \rho), \tag{10}$$

$$a = \frac{1}{2} + (K + 1), \tag{11}$$

$$P_{n_r}^{-a - \frac{1}{2}, -a - \frac{1}{2}}(i \sinh \rho) = \frac{(-a + \frac{1}{2})_{n_r}}{n_r!} {}_2F_1 \left(-n_r, n_r - 2a; -a + \frac{1}{2}; \frac{1 - i \sinh \rho}{2} \right). \tag{12}$$

Here, ${}_2F_1$ is the hyper-geometric function, $(\dots)_t$ is the Pochhammer symbol, ρ is the arc of an open time like hyperbolic geodesic on dS_4 , and n_r denotes the polynomial degree.

Finally, the eigenmodes of the Laplace operator on the three dimensional hypersphere, S^3 , of a hyper-radius R , solve the equation,

$$-\hbar^2 c^2 \Delta_{S^3}(\chi, \theta, \varphi) Y_{K\ell m}(\chi, \theta, \varphi) = \frac{\hbar^2 c^2}{R^2} K(K + 2) Y_{K\ell m}(\chi, \theta, \varphi), \quad K = 0, 1, 2, \dots, \tag{13}$$

with $Y_{K\ell m}(\chi, \theta, \varphi)$ being defined in (8)-(9). The latter equation describes a rigid “dumbbell” (a “rigid rotator” in four Euclidean dimensions) freely hovering around its center of mass, with the ends tracing the great circles of the three dimensional hypersphere, S^3 .

In summarizing, the equations (6) and (13) describe free quantum motions along the respective open time-like and closed space-like geodesics on dS_4 in the sense that the arguments of the wave functions $\phi_{\bar{K}}(\rho)$, and $S_{\ell m}(\chi)$ in the respective equations (11) and (9), change along the arcs, $R\rho$, and $R\chi$, of these geodesics. The open time-like geodesics considered here are hyperbolic deSitter space-times of one less dimension, i.e. dS_3 space-times, while the unique closed space-like geodesic is a three dimensional (hyper)spherical surface S^3 located at the “waste” of the dS_4 hyperboloid.

4 From free quantum motions on dS_4 to one-dimensional stationary wave equations with centrifugal potentials

The free motions on the open time-like–, and the closed space-like dS_4 geodesics can be transformed in their turn into stationary quantum mechanical wave equations with the one-dimensional hyperbolic Pöschl-Teller potential, $V_{\text{PT}}(\rho)$, and the trigonometric Scarf potential, $V_{\text{Sc}}(\chi)$. To do so, the following variable change in (10) has to be performed,

$$F_{Kn_r}(\rho) = \cosh^{\frac{3}{2}} \rho \phi_{\bar{K}}(\rho), \quad \bar{K} = K - n_r, \quad (14)$$

in which case the equation (6) is similarity transformed toward,

$$\begin{aligned} -\hbar^2 c^2 \left[\cosh^{\frac{3}{2}} \rho \Delta_{dS_4}(\rho, \chi, \theta, \varphi) \cosh^{-\frac{3}{2}} \rho \right] &= \left[\cosh^{\frac{3}{2}} \rho Y_{\bar{K}K\ell m}(\rho, \chi, \theta, \varphi) \right] \\ &= -\frac{\hbar^2 c^2}{R^2} \bar{K}(\bar{K} + 3) \left[\cosh^{\frac{3}{2}} \rho Y_{\bar{K}K\ell m}(\rho, \chi, \theta, \varphi) \right]. \end{aligned} \quad (15)$$

In introducing now the notation,

$$\mathcal{H}_{\text{PT}}(\rho, \chi, \theta, \varphi) = \cosh^{\frac{3}{2}} \rho \left[-\hbar^2 c^2 \Delta_{dS_4}(\rho, \chi, \theta, \varphi) \right] \cosh^{-\frac{3}{2}} \rho, \quad (16)$$

for the $[-\hbar^2 c^2 \Delta_{dS_4}(\rho, \chi, \theta, \varphi)]$ Laplacian upon its similarity transformation by the $\cosh^{\frac{3}{2}} \rho$ function, and by the aid of (4) and (7), the equation (15) equivalently rewrites as,

$$\begin{aligned} \mathcal{H}_{\text{PT}}(\rho, \chi, \theta, \varphi) F_{Kn_r}(\rho) Y_{K\ell m}(\chi, \theta, \varphi) &= \frac{\hbar^2 c^2}{R^2} \left[-\frac{d^2}{d\rho^2} + V_{\text{PT}}(\rho) + \frac{3^2}{2^2} \right] F_{Kn_r}(\rho) Y_{K\ell m}(\chi, \theta, \varphi) \\ &= -\frac{\hbar^2 c^2}{R^2} \bar{K}(\bar{K} + 3) F_{Kn_r}(\rho) Y_{K\ell m}(\chi, \theta, \varphi), \end{aligned} \quad (17)$$

with the Pöschl-Teller (PT) potential, $V_{\text{PT}}(\rho)$, being defined as,

$$V_{\text{PT}}(\rho) = \left[(K + 1)^2 - \frac{1}{4} \right] \operatorname{sech}^2 \rho, \quad \rho \in (-\infty, +\infty). \quad (18)$$

Notice that the similarity transformation conserves the $[-\hbar^2 c^2 \Delta_{dS_4}(\rho, \chi, \theta, \varphi)]$ eigenvalues in (6). A way of rephrasing the similarity transformation is to cast it in the form of an intertwining of $\mathcal{H}_{\text{PT}}(\rho, \chi, \theta, \varphi)$ with $[-\hbar^2 c^2 \Delta_{dS_4}(\rho, \chi, \theta, \varphi)]$ by the $\cosh^{\frac{3}{2}} \rho$ function according to,

$$\cosh^{\frac{3}{2}} \rho \mathcal{H}_{\text{PT}}(\rho, \chi, \theta, \varphi) = -\hbar^2 c^2 \Delta_{dS_4}(\rho, \chi, \theta, \varphi) \cosh^{\frac{3}{2}} \rho, \quad (19)$$

and to recall that intertwined Hamiltonians are isospectral [13]. Also notice that the PT potential can be equivalently rewritten to,

$$V_{\text{PT}}(\rho) = \left[(K + 1)^2 - \frac{1}{4} \right] \frac{1}{\cosh^2 \rho} = - \left[(K + 1)^2 - \frac{1}{4} \right] \tanh^2 \rho + \frac{\hbar^2 c^2}{R^2}, \quad (20)$$

where the potential on the r.h.s. is known under the name of the “Higgs oscillator” on dS_4 in reference to the fact that the leading term in the series expansion of $\tanh^2 \rho$ goes as the square, ρ^2 , of the argument meaning that to

leading order the hyperbolic Pöschl-Teller potential behaves as an oscillator. In this sense, free motions on the open hyperbolic time-like geodesics on dS_4 can be viewed as “Higgs” oscillations. In a similar way, through the variable change,

$$\cos \chi Y_{Klm}(\chi, \theta, \varphi) = \cos \chi \mathcal{S}_{n\ell}(\chi) Y_{\ell m}(\theta, \varphi) = U_{n\ell}(\chi) Y_{\ell m}^m(\theta, \varphi), \quad U_{n\ell}(\chi) = \cos \chi \mathcal{S}_{n\ell}(\chi), \quad (21)$$

the equation (13) is similarity transformed toward,

$$\begin{aligned} -\hbar^2 c^2 [\cos \chi \Delta_{S^3}(\chi, \theta, \varphi) \cos^{-1} \chi] &= [\cos \chi Y_{K\ell m}(\chi, \theta, \varphi)] \\ &= \frac{\hbar^2 c^2}{R^2} K(K+2) [\cos \chi Y_{K\ell m}(\chi, \theta, \varphi)]. \end{aligned} \quad (22)$$

In now introducing the notation,

$$\mathcal{H}_{\text{Sc}}(\chi, \theta, \varphi) = -\hbar^2 c^2 [\cos \chi \Delta_{S^3}(\chi, \theta, \varphi) \cos^{-1} \chi], \quad (23)$$

for the $[-\hbar^2 c^2 \Delta_{S^3}(\chi, \theta, \varphi)]$ Laplacian upon its similarity transformation by the $\cos \chi$ function, making use of (8), (9), and (5), and upon some algebraic manipulations, the equation (23) equivalently rewrites as,

$$\begin{aligned} \mathcal{H}_{\text{Sc}}(\chi, \theta, \varphi) U_{\ell n}(\chi) Y_{\ell m}(\theta, \varphi) &= \frac{\hbar^2 c^2}{R^2} \left(-\frac{d^2}{d\chi^2} + V_{\text{Sc}}(\chi) - 1 \right) U_{\ell n}(\chi) Y_{\ell m}(\theta, \varphi) \\ &= \frac{\hbar^2 c^2}{R^2} K(K+2) U_{\ell n}(\chi) Y_{\ell m}(\theta, \varphi), \end{aligned} \quad (24)$$

where the trigonometric Scarf potential, $V_{\text{Sc}}(\chi)$, is given by,

$$V_{\text{Sc}}(\chi) = \ell(\ell+1) \sec^2 \chi, \quad \chi \in \left[-\frac{\pi}{2}, +\frac{\pi}{2} \right]. \quad (25)$$

Same as in the case of the dS_4 Laplacian, also the similarity transformation of the $[-\hbar^2 c^2 \Delta_{S^3}(\chi, \theta, \varphi)]$ Laplacian conserves its eigenvalues in (13) but because these eigenvalues are bound from below, they are referred to as the Laplacian’s “spectrum”.

A way of rephrasing the latter similarity transformation is to cast it in the form of an intertwining by the $\cos \chi$ function of $\mathcal{H}_{\text{Sc}}(\chi, \theta, \varphi)$ and $[-\hbar^2 c^2 \Delta_{S^3}(\chi, \theta, \varphi)]$ according to,

$$\cos \chi \mathcal{H}_{\text{Sc}}(\chi, \theta, \varphi) = -\hbar^2 c^2 \Delta_{S^3}(\chi, \theta, \varphi) \cos \chi, \quad (26)$$

and recall isospectrality of intertwined operators known from the super-symmetric quantum mechanics [13]. The considerations from above show that in terms of one-dimensional wave equations, the free quantum motions along the open time-like, and the closed space-like dS_4 geodesics give in turn rise to the hyperbolic Pöschl-Teller ($V_{\text{PT}}(\rho)$) (equivalently, the Higgs oscillator on dS_4), and the trigonometric Scarf ($V_{\text{Sc}}(\chi)$) potential, which are well known from the super-symmetric quantum mechanics [13] to be exactly solvable. More important, the Hamiltonians $\mathcal{H}_{\text{PT}}(\rho)$ and $\mathcal{H}_{\text{Sc}}(\chi)$, in being intertwined with the dS_4 and S^3 Laplacians, conserve the symmetry of the free geodesic motions which is the conformal symmetry, a reason for which the one dimensional potentials in (18)-(20), and (25) are said to be conformal. Such occurred because the latter potentials correspond to “centrifugal” terms on the respective hyperbolic and hyper-spherical manifolds. In passing now the constant $[-\hbar^2 c^2 / R^2]$ from the l.h.s. in (24) to the r.h.s., and introducing the notation,

$$\left(\mathcal{E}^{(\text{bound})} \right)^2 = \frac{\hbar^2 c^2}{R^2} (K+1)^2, \quad (27)$$

the “spectrum” of the similarity transformed $[-\hbar^2 c^2 \Delta_{S^3}(\chi, \theta, \varphi)]$ Laplacian is obtained in which the eigenvalues, $\left(\mathcal{E}^{(\text{bound})} \right)^2$, now from the perspective of a wave equation, take the place of the squared energies of the states bound within the well. Because the energy depends on the K quantum number alone, and due to the branching rules,

$$\ell \in [0, K], \quad |m| \in [0, \ell], \quad (28)$$

as explained after the equation (6), one immediately notices that the levels of the trigonometric Scarf potential are $\sum_{\ell=0}^{\ell=K} (2\ell + 1) = (K + 1)^2$ -fold degenerate. This type of degeneracy is known from the Hydrogen Atom, where it is attributed to the conformal symmetry of the Maxwell equations, or, more general, to the conformal symmetry of the Relativistic Electrodynamics [14]. Therefore, the eigenmodes of the free quantum motion along the closed S^3 hyper-spherical geodesic on dS_4 fall into a conformal spectrum.

Next we like to attend to the free motion on the open time-like geodesics. The most interesting case in that regard is obtained upon the complexification, $(K + 1) \rightarrow i(K + 1)$, of the parameter defining the potential strength in (18), equivalently, the analytical continuation of the four-dimensional angular momentum to complex values. In this case $\mathcal{V}_{\text{PT}}(\rho)$ is transformed into a barrier and one can consider the complex energies of the resonances transmitted through it. To do so, one has to calculate the transfer scattering matrix, $T(k)$. A scheme for such a calculation has been presented in detail in [15]. The expression obtained along the lines of [15] for the case of our interest reads,

$$T(k) = \frac{\sinh^2 \pi k}{\cosh^2 \pi k + \sinh^2 \pi (K + 1)}. \quad (29)$$

Then the poles, which appear at $k = [(K + 1) + i(n_r - \frac{1}{2})]$, define the complex squared energies, $(\mathcal{E}^{(res)})^2$, of the resonances transmitted through the barrier as,

$$(\mathcal{E}^{(res)})^2 = \frac{\hbar^2 c^2}{R^2} k^2, \quad \text{Im} (\mathcal{E}^{(res)})^2 = 2 \frac{\hbar^2 c^2}{R^2} (K + 1) \left(n_r - \frac{1}{2} \right). \quad (30)$$

$$\text{Re} (\mathcal{E}^{(res)})^2 - c_0 = \frac{\hbar^2 c^2}{R^2} (K + 1)^2, \quad c_0 = -\frac{\hbar^2 c^2}{R^2} \left(n_r - \frac{1}{2} \right)^2 + A^2, \quad (31)$$

where A^2 is some additive ad hoc constant which on long term could be helpful in adjusting the potential parameters to data. Comparison of the latter equation to the “spectral” formula (27) shows that the real parts of the (squared) complex energies, $[\text{Re} (\mathcal{E}^{(res)})^2 - c_0]$, at the poles of $T(k)$, equal the (squared) energies of the states bound within the Scarf well potential. In interpreting this equality as a squared invariant mass M^2 , i.e. in setting

$$M^2 = (\mathcal{E}^{(bound)})^2 = \text{Re} (\mathcal{E}^{(res)})^2 - c_0 = \frac{\hbar^2 c^2}{R^2} (K + 1)^2 = \frac{\hbar^2 c^2}{R^2} (n + \ell + 1)^2, \quad (32)$$

gives rise to linear “trajectories” (linear dependencies of the angular momentum on the mass) of the art,

$$\ell(M, R) = \alpha(R)M - n - 1, \quad \ell = 0, 1, 2, \dots, \quad \ell + n = K, \quad K = 0, 1, 2, \dots \quad (33)$$

with n being the number of nodes in the Gegenbauer polynomials in (9). Notice that the equations (33) and (27) appear dual to each other in sense that “trajectory” formulas are conventionally used to describe resonances transmitted through barriers, while “spectral” formulas are standard to the description of degeneracies of levels bound within well potentials. Within the geometric context consequently pursued through the text, the duality between the mass-formulas in (33) and (27), translates into duality between quantum motions on open hyperbolic time-like, and the closed hyper spherical space-like geodesics on dS_4 .

In conclusion, with the aid of the dS_4 geometry, hypothesized to be the relevant space-time outside the causal Minkowski light cone, and to define the interactions by means of the Green functions to the Laplacians on its geodesic sub-manifolds, a pair of potentials could be identified with the remarkable properties that the energies of the states bound within the well potential equal the real parts of the complex energies of the resonances transmitted to the barrier. Moreover, these energies carry same degeneracies.

In this manner, by virtue of the hypothesis on validity of dS_4 special relativity [6], we were able to establish in [5] a duality between the free quantum motions on open hyperbolic time-like-, and closed hyper-spherical space-like geodesics of the dS_4 space-time. To the end of the article, the physical significance of such a duality will be revealed. Before, in the next section, a deeper insight into the properties of the well potential will be gained.

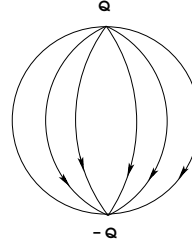


Figure 3: The inevitable charge neutrality of the sphere.

5 Behind the curtains of confinement. Charge neutrality on the hyper-spherical dS_4 geodesic and a conformal color-dipole confining potential

The main point of the present section is to explore consequences of the fact that no single charge can be consistently defined on the sphere [16]. Indeed, the lines pouring out of a charge located at a particular point on this space intersect at the antipodal point, creating there a fictitious opposite charge (see Fig. 3), a reason for which the sphere is necessarily and inevitably charge neutral. In order to satisfy the Gauss theorem [17], that predicts a $\sec^2 \chi$ functional form for the electric field for $\chi \in [-\pi/2, +\pi/2]$, and for the sake of guaranteeing validity of the superposition principle on S^3 , the gradient of the sum of the pod- and anti-pod single charge potentials has to be proportional to $\sec^2 \chi$. The challenge, therefore, is to build up “charge-statics” on S^3 consistent with both the Gauss theorem, and the superposition principle. For the time being the nature of the charge will be left unspecified. For this purpose, one needs to know the Laplacian on the complete space-time $R^1 \otimes S^3$ and then to consider it at constant times. This can be done within the framework of the so called Radial Quantization Technique which prescribes to first Wick-rotate via the complexification, $ct \rightarrow ict$, the Minkowski space time of $(1+3)$ dimensions to 4 Euclidean dimensions, switch to spherical coordinates, and introduce “time” via the logarithm of the S^3 radius [18]. In so doing one finds the following Laplacian,

$$-\left[\frac{\partial^2}{\partial x_4^2} + \frac{\partial^2}{\partial x_1^2} + \frac{\partial^2}{\partial x_2^2} + \frac{\partial^2}{\partial x_3^2} \right] \rightarrow -\left[\frac{1}{R^3} \frac{\partial}{\partial R} R^3 \frac{\partial}{\partial R} - \frac{1}{R^2} \mathcal{K}^2(\chi, \theta, \varphi) \right] \quad (34)$$

$$\xrightarrow{R=e^\tau} e^{2\tau} \left[-\frac{\partial^2}{\partial \tau^2} + (\mathcal{K}^2(\chi, \theta, \varphi) + 1) \right]. \quad (35)$$

The τ parameter is known as “conformal time”. To build up charge-statics, one has to set $\tau=\text{const}$ and to calculate the Green function to the remaining piece, which is the so called conformal Laplacian, $\Delta_{S^3}^1(\chi, \theta, \varphi)$, on S^3 , and is read off from (35) as,

$$\Delta_{S^3}^1(\chi, \theta, \varphi) = \mathcal{K}^2(\chi, \theta, \varphi) + 1, \quad (36)$$

where we have chosen $\tau = 0$, equivalently, $R = 1$. In order to construct the potentials of a charge Q placed at, say, the West “pole”, and of an anti-charge, $(-Q)$, at the East “pole”, one needs to know the respective Green functions, in turn denoted by $\mathcal{G}_{-\frac{\pi}{2}}(\chi)$, and $\mathcal{G}_{+\frac{\pi}{2}}(\chi)$, which have been calculated, among others, in [19], however for $\chi \in [0, \pi]$, and need to be shifted to $\chi \in [-\frac{\pi}{2}, +\frac{\pi}{2}]$. After this small algebraic manipulation, the potentials, constructed from the Green’s function in the standard way known from potential theory [7], emerge as,

$$V_{-\frac{\pi}{2}}(\chi) = Q \mathcal{G}_{-\frac{\pi}{2}}(\chi) = -\frac{Q}{4\pi^2} \left(\chi - \frac{3\pi}{2} \right) \tan \chi, \quad (37)$$

$$V_{+\frac{\pi}{2}}(\chi) = -Q \mathcal{G}_{+\frac{\pi}{2}}(\chi) = -\frac{(-Q)}{4\pi^2} \left(\chi - \frac{\pi}{2} \right) \tan \chi, \quad \chi \in \left[-\frac{\pi}{2}, +\frac{\pi}{2} \right]. \quad (38)$$

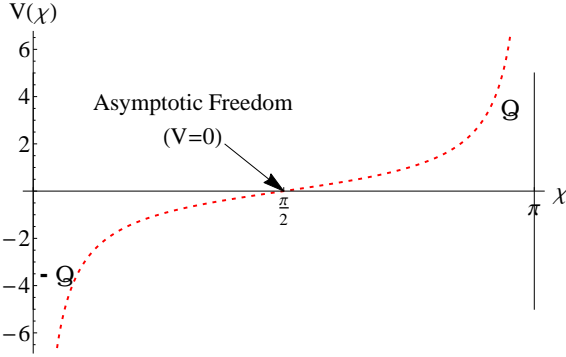


Figure 4: The conformal color dipole confining potential in the $\chi \in [0, \pi]$ parametrization.

In now assuming validity of the superposition principle, one encounters a Charge Dipole (CD) potential to emerge at a point χ on S^3 according to,

$$V_{CD}(\chi) = Q\mathcal{G}_{-\frac{\pi}{2}}(\chi) - Q\mathcal{G}_{+\frac{\pi}{2}}(\chi) = \frac{Q}{4\pi} \tan \chi. \quad (39)$$

The electric field to this dipole is obtained in the standard way through differentiation as,

$$E(\chi) = -\frac{\partial}{\partial \chi} V_{CD}(\chi) = -\frac{Q}{4\pi} \frac{1}{\cos^2 \chi}, \quad \chi \in \left[-\frac{\pi}{2}, +\frac{\pi}{2}\right]. \quad (40)$$

On the one side, this is the precise expression prescribed by the Gauss theorem [17], and on the other, one recognizes in it the functional form of the Scarf well. It is important to notice that $V_{CD}(\chi)$ is conformal because the Green functions have the symmetry of the Laplacian, that on its side has the symmetry of the space-time on which it defines the kinetic energy operator. In effect, the conformal symmetry of the dipole potential provides a further motivation of the conformal symmetry of the trigonometric Scarf well.

More important, the hypothesis of validity of dS_4 special relativity within the interaction domain [6] amounted to the prediction of the new phenomenon of conformally invariant charge neutral systems confined to closed hyper-spherical spaces.

The particular tangent form of the dipole potential is not universal but rather due to the choice of the parametrization for the second polar angle on S^3 , namely, $\chi \in [-\frac{\pi}{2}, +\frac{\pi}{2}]$. This choice is arbitrary and could be changed to $\chi \in [0, \pi]$ in which case the tangent goes into a cotangent and the \sec^2 into \csc^2 . From now onward we shall switch to this very parametrization which turns out to be more suited for physical interpretations, to be presented in the subsequent section. In Fig. 4 we display the dipole potential in the $\chi \in [0, \pi]$ parametrization graphically.

Notice that Q stands for dimension-less charges. In terms of dimensional charges, q , related to Q via,

$$Q = \frac{q}{\sqrt{\hbar c}}, \quad (41)$$

the potential perceived by an other charge $q/\sqrt{\hbar c}$, is,

$$V_{CD}(\chi) = \frac{q^2}{4\pi\hbar c} \cot \chi, \quad \chi \in [0, \pi]. \quad (42)$$

For example, in the case of electrostatic, q is taken as the electron charge, e , in which case the special notation of,

$$\alpha = \frac{e^2}{4\pi\hbar c} \quad (43)$$

known as the fundamental coupling constant of Electrodynamics, is introduced.

The potential in (42) can be applied as a perturbation of the rigid rotator, freely hovering around its center of mass in (13), in which case the following wave equation emerges:

$$\left(-\frac{\hbar^2 c^2}{R^2} \frac{d^2}{d\chi^2} + V_{\text{tRM}}^{(b)}(\chi) \right) U_{\ell n}^{(b)}(\chi) Y_{\ell m}(\theta, \varphi) = \frac{\hbar^2 c^2}{R^2} \left(\epsilon_{\ell n}^{(b)} \right)^2 U_{\ell n}^{(b)}(\chi) Y_{\ell m}(\theta, \varphi), \quad (44)$$

$$V_{\text{tRM}}^{(b)}(\chi) = \frac{\hbar^2 c^2}{R^2} \frac{\ell(\ell+1)}{\sin^2 \chi} - 2 \frac{\hbar^2 c^2}{R^2} b \cot \chi, \quad (45)$$

$$\chi \in [0, \pi]. \quad (46)$$

The potential strength parameter b relates to the charge q as,

$$2b = \frac{q^2}{4\pi\hbar c}, \quad (47)$$

by virtue of our equation (42). In eqs. (44)-(45) one recognizes the one-dimensional wave equation with the trigonometric Rosen-Morse potential which is well known from the super-symmetric quantum mechanics to be exactly solvable [13].

In this way, the cotangent term of the trigonometric Rosen-Morse potential could be derived from the superposition principle on S^3 in combination with the principle of dS_4 special relativity, and could be interpreted as a dipole potential generated by a system consisting of two opposite fundamental charges, to be specified in the following. The centrifugal $\csc^2 \chi$ term of this potential has been generated by the kinetic energy operator on S^3 . In this manner, the complete trigonometric Rosen-Morse potential could be derived from first principles.

The energies, $\frac{\hbar^2 c^2}{R^2} \left(\epsilon_{\ell n}^{(b)} \right)^2$, of the states bound within this potential are given in [13] and read,

$$\frac{\hbar^2 c^2}{R^2} \left(\epsilon_{\ell n}^{(b)} \right)^2 = \frac{\hbar^2 c^2}{R^2} \left[-\frac{b^2}{(K+1)^2} + (K+1)^2 \right], \quad K = \ell + n, \quad K = 0, 1, 2, \dots \quad (48)$$

The “spectral” mass formula resulting then from this potential reads,

$$M^2 = \frac{\hbar^2 c^2}{R^2} \left(\epsilon_{\ell n}^{(b)} \right)^2 = \frac{\hbar^2 c^2}{R^2} (K+1)^2 - \frac{\hbar^2 c^2 b^2}{R^2 (K+1)^2}. \quad (49)$$

To recapitulate, the result is that in hypothesizing validity of dS_4 special relativity [6] outside of the causal Minkowski light cone, it became possible to predict the form of a potential generated by equal numbers of charges and anti-charges locked (confined) on a closed hyper-spherical space. In the next section we will be seeking to identify a physically established phenomenon endowed with such features.

6 Verifying Experimentally. The Mass Distributions of the Unflavored mesons

The phenomenon of charge confinement predicted by the dS_4 special relativity is well known from the theory of strong interactions, the Quantum Chromodynamics (QCD) [20], in which the fundamental matter degrees of freedom, the quarks, are spin-1/2 fermions, endowed with a so called “color” charge. There are three color charges, and three color anti-charges, and the strongly interacting particles, termed to as hadrons, are all color charge neutral. The hadrons of integer spin, the mesons, are constituted of effective degrees of freedom, termed to as “constituent” quarks, and “anti-quarks”, which are also of opposite color charges. Within this context it is legitimate to ask the question as to what extent the scenario developed in the preceding sections and especially of the previous section 5 could apply to the description of the experimentally reported meson masses. The question we are posing is as to what extent the dual “trajectory”- and “spectral” mass formulas in the respective eqs. (33), and (27) are suited for the description of the meson mass dependencies on their angular momenta. Such an analysis has been performed in [5] and we here limit ourselves to only briefly highlight the results.

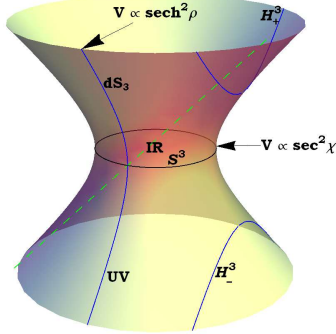


Figure 5: Schematic presentation of the dS_4 space with indicated free motions on the closed space-like geodesic, S^3 , associated with the infrared (IR) and corresponding to the trigonometric Scarf potential well, a $\sec^2\chi$ function for $\chi \in [-\frac{\pi}{2}, +\frac{\pi}{2}]$, and the open hyperbolic time-like dS_3 geodesics, associated asymptotically with the ultraviolet (UV) and corresponding to the Pöschl-Teller potential, a $\operatorname{sech}^2\rho$ function. Straight lines on dS_4 represent three-dimensional Euclidean planes, \mathbf{R}^3 . We note in bypassing that the plane 3D Laplacian gives rise to the regular centrifugal term, $\ell(\ell+1)/r^2$, while its Green function generates the inverse distance, $1/r$ potential. With that, the dS_4 geometry provides the necessary tools not only for the quantum mechanical description of mesons in QCD but also for the Hydrogen Atom in QED.

In [5] we analyzed 71 reported unflavored mesons belonging to the four families of the f_0 , a_0 , π , and η mesons, out of which we here selected for purely illustrative purpose one such family, presented in the Figure 5, namely, the f_0 meson family. Data convincingly confirm the conformal $(K+1)^2$ -fold degeneracy of the levels, as already visible by mere inspection. In addition, their splittings are pretty much like those of the states bound within the trigonometric Scarf potential following from (27), equivalently, like those of the freely hovering four-dimensional rigid rotator in (13). Alternatively, also the dual mass formula in (33) is well applicable. The only splittings which do not come out well from the formulas under discussions are the splittings between the ground states and the first excited states. They can be accounted for by the help of the potential in (39), equivalently, (42).

In order to justify usage of (42) as a perturbation we here suggest to consider mesons as constituted by two types of color-”dumbbells”, one describing a quark-anti-quark configuration, and the other, a gluon-anti-gluon (glueball) configuration. The meson Hamiltonian $\mathcal{H}_M(\chi, \theta, \varphi)$ of such a system can then be approximately separated into a dominant free rotational motion of say, the supposedly light quark-anti-quark pair, described by the Hamiltonian $\mathcal{H}_{SC}(\chi, \theta, \varphi)$ in (23), perturbed by the “residual” color-dipole interaction, $V_{CD}(\chi)$ in (42), attributed to heavier gluon-anti-gluon (glueball) configurations, according to,

$$\mathcal{H}_M(\chi, \theta, \varphi) = \mathcal{H}_{SC}(\chi, \theta, \varphi) + \frac{\hbar^2 c^2}{R^2} V_{CD}(\chi). \quad (50)$$

Such a picture is consistent with the idea of the constituent quarks as effective degrees of freedom, i.e. as fundamental quarks “dressed” by gluons. In adopting $\mathcal{H}_M(\chi, \theta, \varphi)$ as a working hypothesis, one is of course neglecting the perturbation of the glueball by the color-dipole potential generated by the quark-anti-quark pair, and the tensor interaction between the two dipoles [21].

Such corrections may affect the wave functions and become relevant in the calculations of “differential” hadron properties such as transition matrix elements, form-factors etc. As to the spectra, a global characteristic, we demonstrated in [5] that the interacting Hamiltonian in (50) serves quite well the purpose of explaining the gaps between the lowest-, and the first excited states in the f_0 , π , and η families, practically without affecting the rest, a reason for which the perturbation under discussion can be considered as “soft”. More specifically, these

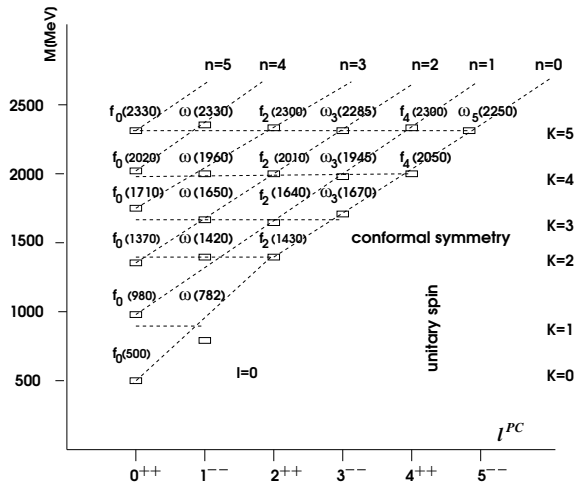


Figure 6: Example for reported [1] mass distributions arranging according to conformal symmetry patterns (graded “brick-wall” spectra) for the case of the f_0 meson excitations. The mesons are depicted on the l^{PC}/M plane, with P and C standing in their turn for the spatial- and charge conjugation parities, and $l \in [0, K]$ according to (28). The relative angular momentum inside the constituent quark–anti-quark pair is identified with the total angular momentum, thus assuming the spins of the quarks to be coupled to zero. The K number on the right encodes besides the four-dimensional angular momentum value in (13) also the number, N , of mesons at a rung as $N = K + 1$. The particles connected by diagonal lines are of steadily growing angular momenta and consequently of alternating P and C parities. The most outer diagonal on the right is referred to as principal trajectory. The integer number n on top of the figure enumerates (from right to left) the accompanying trajectories, placed above the principle one, besides giving the number of nodes of the wave function of the trigonometric Scarf potential in (24). Notice the marked meson groupings at the rungs from $K \geq 2$ onward. Spectra of this type concerning the actual f_0 , and also the π , a_0 , and η mesons have been successfully described in [5] by any one of the two dual mass formulas in (33) (diagonal lines) and (27) (horizontal lines) and identified as a piece of a conformal spectrum. For more details see [5].

gaps have been accounted for in terms of the mass formula in (49), cast in [5] into the form,

$$\begin{aligned} M^2 &= A(R)(K+1)^2 - \frac{B(R)}{(K+1)^2} + C, \\ A(R) &= \frac{\hbar^2 c^2}{R^2}, \quad B(R) = \frac{\hbar^2 c^2}{R^2} b^2, \quad C = \frac{\hbar^2 c^2}{R^2} c_0^2, \end{aligned} \quad (51)$$

where the free additive constant parameter C has been introduced for the purpose to fix the absolute values of the lowest meson masses. In other words, the mass formula in (49) resulted pretty much adequate for the overall satisfactory description on the mass distributions of the unflavored mesons. The restriction to the unflavored mesons was made for the sake of validity of the conformal symmetry, which is to a large amount respected in the sector of the unflavored quarks of comparatively light masses.

Notice that the interpretation of hadrons as states bound within a well potential is adequate near the rest frame, while their interpretation as poles of a scattering matrix is suited beyond rest, up to ultra-relativistic energies. The rest frame is an acceptable approximation at low transferred momenta, in the so called infrared (IR) regime of QCD, while the adequate tool to hadron description at high- up to ultra-high transferred momenta, i.e. close to the ultraviolet regime of QCD, is provided by the scattering matrix. Stated differently, within the QCD context, the quantum motions on the open time-like geodesics will be associated with beyond rest-frame processes up to the ultraviolet regime, while those on the closed space-like geodesic will be associated with near rest frame processes, i.e. with the infrared regime of QCD. In this sense, the achievement of the model advocated in [5] is to have

- associated (to a good approximation) both the infrared and the ultraviolet regimes of QCD with free motions along the respective closed hyper spherical space-like $-$, and the open hyperbolic time-like geodesics on the conformally symmetric dS_4 ,
- established with respect to meson masses description a duality between states bound within a well (IR), and resonances transmitted through a barrier (UV) potentials,
- gained the new understanding about the inevitable color-neutrality of hadrons in the infrared as a consequence of the innate charge-neutrality of the closed hyper-spherical space-like dS_4 geodesic,
- revealed relevance of conformal symmetry in both regimes.

In summary, quantum motion in the infrared regime is close to a free “hovering” of a quark–anti-quark “dumbbell” around its center of mass, with the ends tracing the closed hyper-spherical space-like geodesic of the dS_4 space-time. Instead, up to the ultraviolet, mesons are color-neutral resonances transmitted through a barrier, obtained by analytical continuation of the four-dimensional angular momentum that characterizes the free motions along open time-like dS_4 geodesics (see Fig. 7). However, color-neutrality in the ultraviolet occurs by virtue of the dual meson description and is not inevitable there because on open space-times free charges can exist. To the amount the dS_4 space-time is conformally symmetric, so are the quantum motions on its geodesics.

7 Extracting the running coupling constant from the experimentally observed mass distributions of the unflavored mesons

As already mentioned above, the fundamental matter degrees of freedom in the theory of strong interaction, the Quantum Chromodynamics, the quarks, can carry three different color charges. The color charge, denoted by $g(Q^2)$, depends on the negative square of transferred space-like four-momentum, Q^2 , and the related fundamental coupling in QCD, $\alpha_s(Q^2)$, is defined in analogy to (43) as

$$\alpha_s(Q^2) = \frac{g^2(Q^2)}{4\pi\hbar c}, \quad Q^2 \geq 0, \quad (52)$$

and changes with Q^2 , a reason for which is termed to as “running”. In fitting the meson spectra by the mass formula in (49), an estimate for $g(Q^2)$ and therefore for the running coupling constant of QCD, $\alpha_s(Q^2)$, can be obtained by virtue of our equation (47). However, in the latter, in case of color charges, their number, N_c , has to be accounted for, leading to,

$$2b = \frac{g^2(Q^2)}{4\pi\hbar c} N_c = \alpha_s(Q^2) N_c, \quad (53)$$

trajectory	R	b	c_0	σ^2 [GeV] ⁴	$\frac{\alpha_s}{\pi}$
π for $K \geq 0$	0.58 fm	3.586	3.468	0.09455534 GeV ⁴	0.76
f_0 for $K \geq 0$	0.58 fm	3.180	3.381	0.04359349 GeV ⁴	0.67
η for $K \geq 0$	0.58 fm	2.744	3.279	0.04327266 GeV ⁴	0.58
a_0 for $K \geq 1$	0.58 fm	5.176	3.500	0.05591601 GeV ⁴	1.098
f_1 for $K \geq 0$	0.58 fm	3.788	5.125	0.16528390 GeV ⁴	0.80
a_1 for $K \geq 0$	0.58 fm	3.726	5.071	0.09191531 GeV ⁴	0.79

Table 1: Parameters of the least square fit to the 89 meson masses distributed over the six trajectories indicated to the very left, in employing the mass formula in (51). The last column contains the value of the extracted strong coupling constant, α_s/π , identified by the equation (53). The strong coupling extracted from the a_0 family is notably higher than the values extracted from the other families and is due to the absence of the $K = 0$ state. The a_0 spectrum begins directly with the $K = 1$ level containing the significantly mass-split $a_0(980)$ and $\rho(770)$ mesons (see [5] for details), a circumstance that prejudices the fit in this sector. Had we assumed the mass of the missing state to equal the mass of the $f_0(500)$ meson, same α_s/π value would have been extracted from both families. We rather opt for dropping the value under discussion from the final statement. The explicit expression of σ^2 reads $\sigma^2 = \frac{(\sum \Delta M^2)^2}{N-1}$, where ΔM^2 stands for the deviation of the squared experimental from the squared theoretical masses, and N is the number of states in a family.

and pretty much in parallel to the amplitude $Z\alpha$ of the Coulomb potential following from QED. In the following we first complement the analyzes of the mass distributions of the four meson families previously studied in [5] (71 masses) by two more meson families, the ones of the f_1 , and a_1 mesons, which contribute 18 more masses. Afterwards we extract for the first time the α_s value from the data set on the meson masses, constituted by a total of 89 masses. Compared to the f_0 , η , π , a_0 mesons, analyzed in [5], less is known about the f_1 and a_1 mesons. The compiled data on the last two families are presented in Fig. 7. It needs to be said that only the $a_1(1260)$, $a_1(1640)$, and $f_1(1285)$ mesons are contained in the Summary Table of the Meson Particle Listings in [1] meaning that their existence is considered as fully reliable. All the other particles in Fig. 7 are either included in the Meson Particle Listings, or into the list of the less reliably established particles referred to as “Further States”. We here favored the $f_1(1510)$ meson as the first excited state of $f_1(1285)$ over the $f_1(1420)$ state from the Summary Table. In this way we are suggesting that the internal $f_1(1510)$ structure may be closer to a quark-anti-quark “dumbbell” perturbed by the gluon-anti-gluon (glueball) color dipole potential than the $f_1(1420)$ internal structure, which may contain strange-anti-strange quarks. Our point is that our conformal symmetry classification scheme, in needing states omitted from the Summary Table, provides an additional legitimization to their observation and strengthen their status. Same as in [5], we employed the mass formula in (51) to perform a least square fit to the meson mass distributions in Fig. 7. The results on the three parameters, the hyper-sphere radius, R , and the two dimensionless parameters b , and c_0 in (51), are listed in the columns second to fourth of Table 1, together with the same information regarding the f_0 , η , π , and a_0 families, earlier obtained in [5]. The fifth column contains the average deviation values of the corresponding fits, while in the last column we present the values of the strong coupling constant, α_s , of QCD (normalized to π) which we extracted by virtue of our formula (53). The Table shows that the α_s/π values, in varying in the interval, $0.58 \geq \alpha_s/\pi \leq 0.80$, remain significantly less than 1, and in complete agreement with data reported in [8], whose principle result is that the strong coupling constant tends to approach a fixed value in the infrared, thus opening up a so called “conformal window” and thereby hinting on relevance of conformal symmetry in the infrared. Finally, it is important to emphasize that the infrared $(-\mathcal{Q})\mathcal{G}_{\frac{\pi}{2}}(\chi)$ single-color potential in (38) relates by argument shift, followed by the complexification

$$(-\mathcal{Q})\mathcal{G}_{\frac{\pi}{2}}(\chi) \xrightarrow{\chi \rightarrow \chi' + \frac{\pi}{2}} (-\mathcal{Q})\frac{1}{4\pi^2} [-\chi' \cot \chi'] \xrightarrow{\cot \chi' \rightarrow \cot i\chi'} (-\mathcal{Q})\frac{1}{4\pi^2} [-\rho \coth \rho], \quad (54)$$

and coincides with the expression giving the potential generated in the ultraviolet by the color charge, $-\mathcal{Q} = \frac{g}{\sqrt{h_c}}$, of a stopped fast quark, emitting soft gluons at a cusp [22], and in support of the IR-UV duality advocated in [5] and here. The Wilson loop calculation of such a potential, in making use of radial quantization, is practically equivalent to our calculation in section 5.

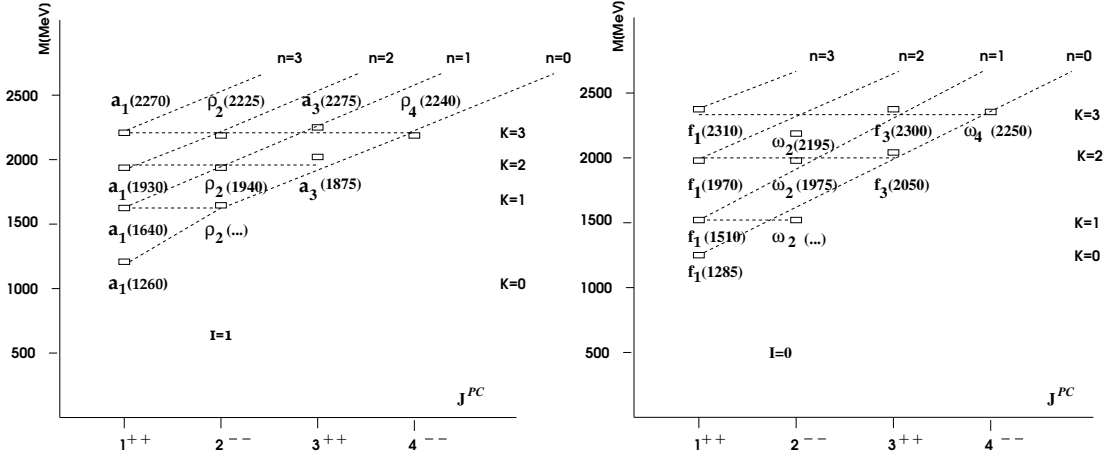


Figure 7: The excitations of the isovector $a_1(1260)$ meson (left) and the isoscalar $f_1(1285)$ meson (right). ‘‘Missing’’ states are denoted by (...). Here, J is the total angular momentum value of the quark-diquark system obtained from coupling the total spin $S = 1$, to the relative angular momentum, $\ell = 0, 1, 2, 3$. Recall the definition of $K = n + \ell$ in (33). Other notations same as in Fig. 5.

8 Summary and outlook

Our analyzes show that the experimentally reported conformal symmetry patterns of the light flavored meson mass distributions are well modelled by

- a conformal dS_4 space-time geometry outside of the Minkowskian causal Light Cone and in accord with the hypothesis on dS_4 special relativity of [6],
- interactions in the infrared regime of QCD understood as virtual quantum motions on the closed space-like hyper-spherical geodesic S^3 on dS_4 , where quark systems are inevitably and necessarily colorless,
- hadrons viewed in the infrared as color-anti-color ‘‘dumbbells’’ in free conformal four-dimensional rotation, corresponding to the centrifugal $\ell(\ell+1)\csc^2\chi$ potential, or motions slightly perturbed by the also conformal color-dipole potential, $(-2b \cot \chi)$ (attributed to glueballs) whose magnitude is proportional to the strong coupling constant α_s by virtue of (53), a circumstance that allowed us to extract the α_s value from data on the meson masses in accord with data,
- relevance of conformal symmetry in both the extreme regimes of QCD.

Thus, either the external conformal symmetry, via dS_4 special relativity, motivates the internal color gauge group, $SU(3)_C/Z_3$, or, vice versa. However, at open spaces, such as the causal patches, space-time locus-es of bubble walls nucleated in dS_4 , where no charge-neutrality is required, color could be released within this scenario and become observable. Our findings favor conformal $(2 + 4)$ space-time over the Minkowskian $(1 + 3)$ space-time, with the extra dimensions, a frozen second time-, and an additional space-like dimension, showing up off-shell. In effect, the description of the simplest composite (two-body) systems in QCD, the mesons, have been put at a comparable footing with the description of the simplest composite (two-body) system in QED, the H atom. The correspondence between the strong and the Coulomb potential (here for an adimensional radial distance, r ,) has been found as,

$$\text{QED} : \quad -Z\alpha \left(\frac{1}{r} \right) \longleftrightarrow -N_c \alpha_s \cot \chi, \quad \text{QCD.} \quad (55)$$

The scheme is Fourier transformable and can be re-formulated in momentum space. Models of this type are free from infrared divergences [22], a reason for which considering QCD on closed spaces is appealing (also see [4] for further reading). To the best of our knowledge, the model under discussion is so far the only one which allows to estimate the fundamental coupling constant of QCD from analyzes of global (integral) properties

of hadron systems such as spectra. Usually, these values are extracted from data on the spin structure function [8]. Our major conclusion is that behind the curtains of conformal symmetry and color-confinement in QCD one encounters the deSitter dS_4 special relativity as a string-puller.

References

- [1] K. A. Olive *et al.* (Particle Data Group), Review of Particle Physics, Chinese Physics C **38** 090001 (2014) and 2015 update.
- [2] Fayyazuddin and Riazuddin, *A Modern Introduction to Particle Physics*, 2nd edition, (World Scientific, Singapore, 2000)
- [3] A. Chodos, R.L. Jaffe, K. Johnson, and C. B. Thron, Phys. Rev. D **10** (1974) 2599.
- [4] D. Kharzeev, E. Levin, and K. Tuchin, Phys. Rev. D **70** (2004) 054005 .
- [5] M. Kirchbach and C. B. Compean, Eur.Phys.J. A **52** (2016) 210.
- [6] R. Aldrovandi, J. P. Beltrán Almeida, and J. G. Pereira, Class. Quant. Grav. **24** (2007) 1385.
- [7] O. D. Kellogg, *Foundations of Potential Theory* (Dover, New York, 1953).
- [8] A. Deur, V. Burkert, J. P. Chen, and W. Korsch, Phys. Lett. **665** (2008) 349.
- [9] A. Einstein, Annalen der Physik **IV** (17) (1905) 891.
- [10] Slava Rychkov, *EPFL Lectures on Conformal Field Theory in $D \geq 3$ dimensions*, E-print arXiv:1601.05000[hep-th].
- [11] Yoonbai Kim, Chae Young Oh, and Namil Park, J. Korean Phys. Soc. **42** (2003) 573 .
- [12] Andrew Pressley, *Elementary Differential Geometry* (Springer, London Dordrecht Heidelberg New York, 2012).
- [13] F. Cooper, A. Khare, and U. P. Sukhatme, *Supersymmetry in Quantum Mechanics* (World Scientific, Singapore, 2001).
- [14] H. Bateman, Proc. London Math. Soc. (ser. 2) **7** (1909) 70.
- [15] D. Cevik, M. Gadella, S. Kuru, and J. Negro, Phys. Lett. A **380** (2016) 1600.
- [16] L. D. Landau and E. M. Lifschitz, *The Classical Theory of Fields*, Vol. 2 of A Course of Theoretical Physics, 3d edition (Pergamon Press 1971) p.335.
- [17] Pouria Pedram, Am. J. Phys. **78** (2010) 403.
- [18] S. Fubini, A. J. Hanson, and R. Jackiw, Phys. Rev. D **7** (1972) 1732.
- [19] B. Alertz, Ann.Inst.Henri Poincaré, **53** (1990) 319.
- [20] Kerson Huang, *Quarks, Leptons and Gauge Fields* (World Scientific, Singapore, 1982).
- [21] J.-M. Gaillol and M. Trulsson, J. Chem. Phys. **141** (2014) 124111.
- [22] A. V. Belitsky, A. S. Gorsky, and G. P. Korchemsky, Nucl. Phys. B **67** (2003) 3.